



*1D-to-3D transition of phonon heat conduction in polyethylene using molecular dynamics simulations*

The MIT Faculty has made this article openly available. **Please share** how this access benefits you. Your story matters.

<b>Citation</b>	Henry, Asegun et al. "1D-to-3D transition of phonon heat conduction in polyethylene using molecular dynamics simulations." Physical Review B 82.14 (2010) : n. pag. © 2010 The American Physical Society
<b>As Published</b>	<a href="http://dx.doi.org/10.1103/PhysRevB.82.144308">http://dx.doi.org/10.1103/PhysRevB.82.144308</a>
<b>Publisher</b>	American Physical Society
<b>Version</b>	Final published version
<b>Accessed</b>	Sat Aug 19 05:24:44 EDT 2017
<b>Citable Link</b>	<a href="http://hdl.handle.net/1721.1/63142">http://hdl.handle.net/1721.1/63142</a>
<b>Terms of Use</b>	Article is made available in accordance with the publisher's policy and may be subject to US copyright law. Please refer to the publisher's site for terms of use.
<b>Detailed Terms</b>	

# 1D-to-3D transition of phonon heat conduction in polyethylene using molecular dynamics simulations

Asegun Henry,<sup>1,2,\*</sup> Gang Chen,<sup>1,†</sup> Steven J. Plimpton,<sup>3</sup> and Aidan Thompson<sup>3</sup>

<sup>1</sup>*Department of Mechanical Engineering, Massachusetts Institute of Technology, 77 Massachusetts Avenue, Cambridge, Massachusetts 02139, USA*

<sup>2</sup>*Georgia Institute of Technology, George W. Woodruff School of Mechanical Engineering, 801 Ferst Drive, Atlanta, Georgia 30332, USA*

<sup>3</sup>*Sandia National Laboratories, Albuquerque, New Mexico 87185-1110, USA*

(Received 2 August 2010; published 26 October 2010)

The thermal conductivity of nanostructures generally decreases with decreasing size because of classical size effects. The axial thermal conductivity of polymer chain lattices, however, can exhibit the opposite trend, because of reduced chain-chain anharmonic scattering. This unique feature gives rise to an interesting one-dimensional-to-three-dimensional transition in phonon transport. We study this transition by calculating the thermal conductivity of polyethylene with molecular dynamics simulations. The results are important for designing inexpensive high thermal-conductivity polymers.

DOI: [10.1103/PhysRevB.82.144308](https://doi.org/10.1103/PhysRevB.82.144308)

PACS number(s): 65.40.-b, 66.10.cd, 66.30.hk, 63.20.-e

Classical size effects on the thermal conductivity of thin-films, nanowires, superlattices, and nanocomposites have received significant attention both theoretically and experimentally, with reasonable agreement.<sup>1-4</sup> The basic picture depicted by this area of research is that shrinking the size of crystalline materials results in lower thermal conductivity because of increased phonon scattering at boundaries. Although size reduction generally leads to lower thermal conductivity, some nanostructures such as carbon nanotubes<sup>5-7</sup> and polymer chains<sup>8-11</sup> exhibit starkly contrasting behavior and have high thermal conductivity. Using molecular dynamics simulations, Moreland *et al.*<sup>12</sup> predicted that the thermal conductivity of diamond nanowires is much smaller than that of carbon nanotubes of comparable diameter. This is because a nanotube is one-dimensional (1D) in the sense that there is only one dimension of spatial periodicity in the atomic arrangement, which occurs along the tube axis. This reduction in dimensionality limits the number of phonon scattering events that can satisfy energy and momentum conservation, which subsequently leads to longer phonon mean free paths and higher thermal conductivity.

In fact, in the 1950s, Fermi, Pasta and Ulam<sup>13</sup> discovered that a 1D lattice chain can have divergent (infinite) thermal conductivity when anharmonic interactions (nonlinear forces) are included. Their pioneering work inspired extensive literature on anomalous heat conduction in 1D lattices.<sup>10,14-19</sup> More recently, molecular dynamics simulations have shown that an individual polyethylene chain can also have divergent thermal conductivity.<sup>8,10</sup> Bulk polyethylene, on the other hand, has a low thermal conductivity  $\sim 0.35$  W/m K,<sup>9,20</sup> because the chains are entangled and their orientations are highly disordered.

The transition from high thermal conductivity in a single polymer chain to low thermal conductivity in bulk polymers is quite interesting from both a fundamental and practical stand point. Experiments on mechanically stretched bulk polyethylene<sup>9,21</sup> report thermal conductivities as high as  $\sim 42$  W/m K (comparable to that of steel) along the stretching direction<sup>9</sup> due to greater alignment of the constituent chains. Although we anticipate that the thermal contact resis-

tance between chains will play a crucial role, anharmonic interactions between chains can lead to increased phonon-phonon scattering, which can diminish the high/diverging thermal-conductivity of individual chains. From a practical stand point, it is important to understand this effect for the design and structural optimization of inexpensive high thermal-conductivity polymers.<sup>9,11</sup> From a fundamental perspective, the strongly anisotropic bond chemistry (i.e., stiff covalent bonding along the chain backbone versus weak van der Waals bonding in the lateral directions) gives rise to an interesting size effect on thermal conductivity. A similar effect was reported by Berber, Kwon, and Tomanek<sup>5</sup> who observed an order of magnitude decrease in thermal conductivity when comparing a single [two-dimensional (2D)] graphene sheet to [three-dimensional (3D)] graphite. Similar observations were also reported by Nika *et al.*<sup>22</sup> More recently, this 2D-3D transition was observed experimentally by comparing the thermal conductivity of sheets of graphene with one to four layers.<sup>23,24</sup> Here we provide a systematic investigation of this phenomenon in the context of a polymer chain lattice, by studying how the thermal conductivity changes as we gradually build a lattice from 1D as a single chain, to 2D as a single sheet, to 3D as a single crystal.

In polyethylene, the weakly attractive van der Waals forces between polymer chains give rise to a lattice structure in both 2D and 3D. This feature, allows for observation of both a 1D-to-2D and 2D-to-3D transition in phonon transport. Starting from a single polyethylene chain, which is expected to have high thermal conductivity,<sup>8,10</sup> we anticipate a transition to 2D behavior as more chains are added to form a single lattice plane (1D-to-2D transition). The 2D lattice plane should then exhibit lower thermal conductivity, as a result of anharmonic scattering induced by neighboring chains. A second transition from 2D-to-3D is also expected as additional lattice planes are stacked, leading to even more interchain anharmonic scattering, which should lower the thermal conductivity even further.<sup>23</sup> The strongly anisotropic phonon transport in polymer chain lattices<sup>9</sup> can therefore cause the axial thermal conductivity to increase with decreasing crystal size, which is the opposite trend observed in most nanostructures and bulk materials.

TABLE I. Simulation domain details.

Phonon transport	Molecules stacked in $x$ direction	Periodic boundaries in $x$ direction	Layers stacked in $y$ direction	Periodic boundaries in $y$ direction	Number of molecules	Number of atoms
1D	1	No	1	No	1	240
1D-2D	2	No	1	No	2	480
1D-2D	4	No	1	No	4	960
1D-2D	6	No	1	No	6	1440
1D-2D	12	No	1	No	12	2880
2D	12	Yes	1	No	12	2880
2D-3D	6	Yes	1	No	6	1440
2D-3D	6	Yes	2	No	12	2880
2D-3D	6	Yes	3	No	18	4320
2D-3D	6	Yes	4	No	24	5760
2D-3D	6	Yes	5	No	30	7200
3D	6	Yes	5	Yes	30	7200

In this paper we use molecular dynamics simulations to predict the thermal conductivity of polyethylene at each stage of the anticipated 1D-to-3D transition. Here, we are principally interested in isolating the effects of anharmonic phonon-phonon scattering. We do not include other potential scattering mechanisms that can further reduce the thermal conductivity, such as defects and interface/boundary resistance between chain ends. To study this 1D-to-3D transition we employ the widely used Green-Kubo approach,<sup>25–27</sup> which is based on linear response theory, where the axial thermal conductivity is given by

$$\kappa = \frac{V}{k_B T^2} \int_0^\infty \langle Q_z(t) Q_z(t+t') \rangle dt', \quad (1)$$

where  $k_B$  is Boltzmann's constant,  $T$  is the system temperature,  $V$  is the system volume and  $\langle Q_z(t) Q_z(t+t') \rangle$  is the heat flux autocorrelation (HFAC) function. Hardy's expression for the heat flux operator<sup>28</sup> was used to determine the axial  $z$  component of the heat flux,  $Q_z(t)$ , which is directed along the polyethylene chain backbone. This equilibrium molecular dynamics approach has shown good agreement with experiments<sup>2,11,29–32</sup> and is used here to examine how the axial thermal conductivity of each group of interacting polyethylene chains decreases as additional chains are added.

In order to study the proposed 1D-to-3D transition, we require a model that can describe both intramolecular (covalent) and intermolecular (van der Waals) interactions. The most crucial aspect of atomistic simulation is having an accurate description of the interatomic forces. Although *ab initio* methods are very accurate, their computational cost currently renders them unfeasible for studying polyethylene at the length scales of interest. Empirical potentials, on the other hand, are much less expensive, but can suffer from inaccuracy. For hydrocarbon systems, such as polyethylene, the second generation Brenner potential<sup>33</sup> is the most widely used, and has shown good agreement with experiments on the thermal conductivity of diamond.<sup>29</sup> This highly successful potential, however, only describes covalent interactions

for atoms separated by less than 2 Å. Stuart *et al.*<sup>34</sup> built on Brenner's pioneering work and alleviated this constraint by adding a Lennard-Jones term, which has a large cutoff, as well as a four-body potential for preferred dihedral angles in polymeric systems. The resulting adaptive intermolecular reactive empirical bond order potential<sup>34</sup> (AIREBO) was chosen for the present investigation because it has a Lennard-Jones term that allows neighboring chain molecules to interact, leading to enhanced phonon-phonon scattering. The sixth power dependence of this van der Waals chain-chain interaction is well established.<sup>34</sup> The key point of this study was to examine the extent to which the weaker intermolecular interactions could interfere with the much stronger intramolecular covalent forces, in order to induce phonon-phonon scattering and reduce thermal conductivity.

Parallel molecular dynamics simulations were used because of the requisite nanometer length scales and nanosecond time scales. In this investigation, the AIREBO potential<sup>34</sup> was implemented in the LAMMPS parallel molecular dynamics package developed at Sandia National Laboratories.<sup>35</sup> The simulations described in this report were run using Sandia's high-performance computing facilities, with processor grids ranging from 2–30 processors. To investigate the 1D-to-3D phonon transport transition, twelve different systems of polyethylene chains were studied by varying the usage of periodic boundary conditions, as listed in Table I. In all 12 cases each molecular chain consisted of 80 carbon atoms (40 unit cells long).<sup>8,10</sup> All simulations employed periodic boundary conditions along the length of the chains in the  $z$  direction; the use of periodic boundaries in the other two directions is indicated in Table I. Periodic boundary conditions were used in the  $x$  direction to represent infinite sheets, and additionally in the  $y$  direction to represent bulk material. Figure 1 shows the equilibrium atomic positions associated with a 1D single chain, 2D single sheet (single lattice plane), and the 3D bulk single crystal while the arrows denote the  $x$  and  $y$  directions where the usage of periodic boundary conditions was varied.

As mentioned, the AIREBO potential<sup>34</sup> allows for a user-specified cutoff in the Lennard-Jones term. In the present

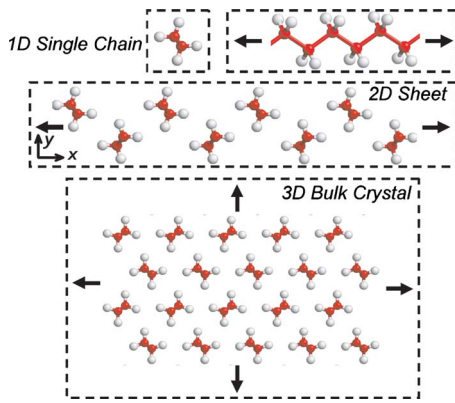


FIG. 1. (Color online) Cross-sectional depiction of the 1D, 2D, and 3D chain lattice structures.

work, this cutoff was chosen as three times the minimum energy separation  $\sigma_{ij}$  for the Lennard-Jones interaction of the associated atomic species, which corresponded to  $\sim 10$  Å for carbon-carbon interactions and  $\sim 8$  Å for hydrogen-hydrogen interactions. This allowed for chain-chain interactions between third and fourth nearest-neighboring chain molecules. The minimum-energy positions for each chain in the zigzag conformation and bulk orthorhombic crystalline structure<sup>36</sup> were obtained by standard conjugate-gradient energy-minimization methods in LAMMPS. The resulting unit cell size was  $(7.13 \text{ Å} \times 5.01 \text{ Å} \times 2.55 \text{ Å})$ , which is within 4% of the values measured experimentally.<sup>37</sup> All simulations were run at constant energy, volume, and number of atoms. Preliminary testing indicated that a 0.25 fs time step was needed for good energy conservation  $\delta E/E_0 < .0001\%$  over the course of several nanoseconds of simulation time.<sup>8,10</sup> Other preliminary thermal-conductivity calculations indicated that 10 ns of simulation time were required for thermal conductivity convergence within  $\sim 30\%$ .<sup>8,10</sup> For each case listed in Table I, ten independent simulations were run. The simulations were started with all atoms at their equilibrium (minimum energy) positions and random velocities corresponding to a quantum corrected temperature of 300 K.<sup>8,38</sup> This choice of temperature definition corresponds to  $\sim 85$  K, if the more standard definition based on equipartition is used. It should be emphasized here that the primary objective of this study is to probe the qualitative trends associated with a 1D-to-3D transition in phonon transport. Therefore the actual thermal-conductivity values obtained herein are most meaningful with respect to each other, as opposed to taking primary interest in comparing these results to experiments, which has already been pursued elsewhere.<sup>11</sup>

The HFAC in all simulations exhibited large oscillations around 56 THz, which are attributed to the carbon-carbon bending modes.<sup>8,10,39</sup> Although these oscillations are large and remain correlated for a very long time, they do not contribute to the thermal transport because they are symmetric about zero. These optical mode vibrations essentially amount to a background overlay, as it is well known that optical modes make up a significant portion of the energy content but are insignificant heat carriers due to their low group velocities.<sup>2,8,39-41</sup> Thus, in Fig. 2 we show the HFAC after these strong oscillations have been filtered out so that the

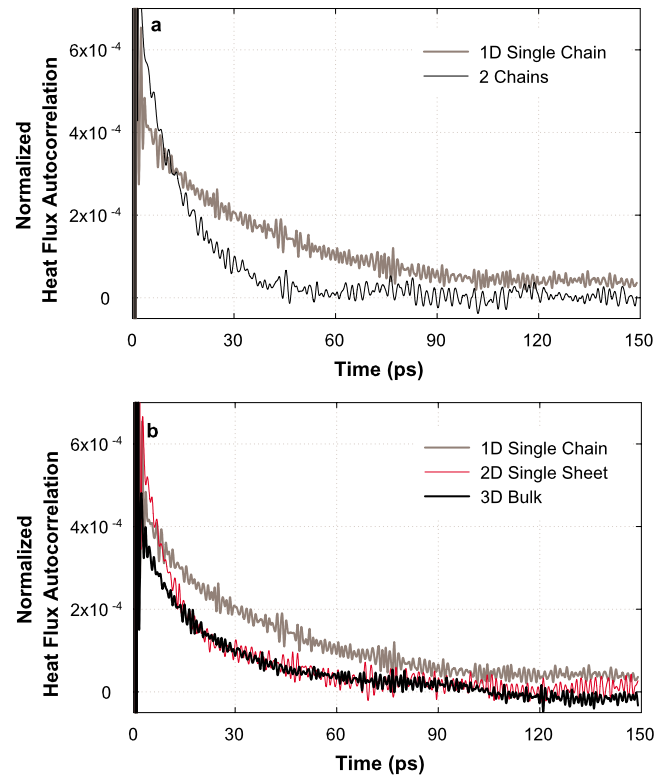


FIG. 2. (Color online) Normalized HFAC functions. (a) and (b) show the average HFAC function for 10 independent simulations of the 1D, 2D, and 3D cases in Table I, as well as the second case with two chains. (b) shows the long time behavior of the HFAC functions for the 1D, 2D, and 3D cases in Table I. In both (a) and (b) the data has been smoothed over 1ps intervals to filter out high frequency oscillations for clearer representation of the decaying features.

decaying features of the autocorrelations can be studied.

For comparison, Fig. 2(a) shows how the HFAC function decays for a single chain and two chains. In a single chain, there are modes that carry heat and can remain correlated indefinitely, leading to divergence.<sup>8,10</sup> When a second chain is added, however, there are two consequences. First, the van der Waals interaction perturbs the modes in each chain that have the potential to remain correlated, which is evidenced by the fact that the decay rate increases significantly in Fig. 2(a), and the thermal conductivity is convergent in all simulations of two chains. Second, there are additional low-frequency vibrations that occur between the two chains, which may explain why the HFAC is slightly higher at very short times, when the vibrations are still correlated. Nonetheless, the comparison suggests that the transition from 1D-to-2D behavior is sharp and chain-chain phonon-phonon scattering is substantial when only two chains are present. Figure 2(b) shows how the decay of the HFAC function changes for the 1D chain, 2D sheet, and 3D bulk cases, shown in Table I. Here the 1D case has a long tail, which is associated with the divergence<sup>8,10</sup> while the 2D and 3D cases on the other hand do not exhibit this feature and decay more rapidly. This is consistent with purely diffusive behavior and can be seen by the similarity between the 2D and 3D behavior after 15 ps.



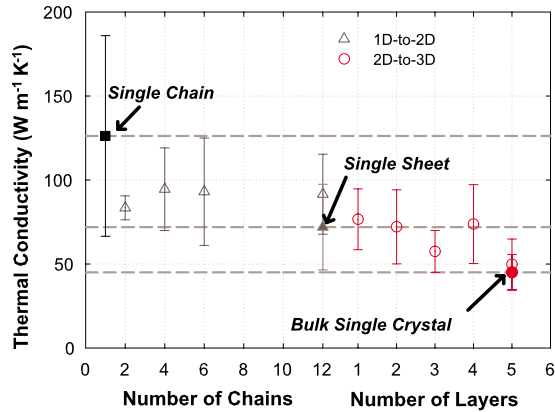


FIG. 3. (Color online) Thermal conductivity results from the Green-Kubo analysis, showing the 1D-2D (left) and 2D-3D (right) transitions. The left portion of the horizontal axis is given in number of molecular chains for the 1D-2D transition while the right portion of the horizontal axis is given in terms of the number of 2D layers being stacked for the 2D-3D transition. Dashed lines indicate the values obtained for the 1D single chain limit, the 2D sheet limit, and the 3D bulk crystal limit, which show the increasing trend with decreased dimensionality.

The results in Fig. 3 show the thermal conductivity values obtained for all 12 cases described in Table I. This figure shows the full 1D-2D and 2D-3D transitions with respect to the number of chains or layers in the corresponding dimension. Numerical integration of the HFAC functions after several nanoseconds exhibited oscillations due to cumulative noise associated with the longitudinal acoustic phonons, which are the most dominant heat carriers.<sup>8,10</sup> As a result, the  $\infty$  integration limit in Eq. (1), was truncated to 500 ps, which sufficiently captures the autocorrelation decay for the 2D and 3D cases, as shown in Fig. 2(b). For the 1D cases, this truncation captures the normal diffusive transport behavior exhibited in convergent simulations, and prevents the persistent HFAC functions that lead to divergent thermal conductivity from offsetting the results. Each point in Fig. 3 therefore represents the average thermal conductivity of all ten independent simulations while the error bars show the standard deviation. Despite the spread in the results, the 1D-to-3D transition and overall trend of decreasing thermal conductivity with increasing size is nonetheless apparent. The results of Fig. 3 also show that the transition from 1D-2D is sharper than the transition from 2D-3D. The single chain thermal conductivity is large, as expected.<sup>8,10</sup> However, when two chains are allowed to interact the thermal conductivity decreases by  $\sim 40\%$ , which is also evident from Fig. 2(a). As more chains are added to form a single layer of chains the thermal conductivity does not change as drastically. Once periodic boundary conditions are employed in 2D, the tran-

sition to 3D is less abrupt, and the thermal conductivity decreases from the planar limit by another  $\sim 30\%$ . Once five layers of chains have been stacked, Fig. 3 shows that the thermal conductivity is quite close to that of the bulk value predicted when periodic boundaries are employed in all three dimensions. This result is consistent with the findings reported by Ghosh *et al.*, where it was observed that only four layers of graphene (2D) were required to approach the thermal conductivity of high-quality bulk graphite (3D).<sup>23</sup>

Intuitively we know that whenever a new mode is introduced into a system, two competing effects are manifested. For one, an additional mode can contribute to the energy content of the material as measured in the specific heat and it can carry heat if the energy propagation velocity is significant, thus serving to increase the thermal conductivity. The secondary effect is that adding another mode to a system also opens up new routes for phonon-phonon scattering, which serve to decrease the thermal conductivity. The net effect of adding a mode to a system depends on the sum of these two effects and is evidenced by whether or not the thermal conductivity increases or decreases. In the case of polymer chain lattices, we know that when starting from a single chain, as more molecular chains are added to the simulation domain, new modes are added to the system and begin propagating in the perpendicular directions and at intermediate angles in between.<sup>42</sup> These phonons contribute to the axial thermal conductivity by carrying heat, but can also detract from the high thermal conductivity of each individual chain, by scattering the most efficient heat carrying phonons, which propagate along each chain's carbon backbone. The vital characteristic that allows for the 1D-to-3D transition shown in Fig. 3, is that these phonons detract from the axial heat conduction more than they can contribute, thus reducing the net thermal conductivity. The fact that the thermal conductivity decreases as more modes are added (1D-to-2D-to-3D), confirms that the secondary effect of increased scattering is stronger than the primary effect of having additional heat carriers. Our results therefore show that the anharmonic scattering induced by weak van der Waals forces can cause significant attenuation of modes propagating along the stiff covalently bonded polymer chain backbone [Fig. 2(a)]. This provides important quantitative insight into heat conduction in polymer lattices, which will be necessary for designing and manufacturing low-cost high thermal-conductivity polymers.<sup>9,11</sup>

We acknowledge funding resources provided by the DOE to A. H., computing resources provided by Sandia National Laboratories, and NSF under Grant No. CBET-0755825. Our implementation of the AIREBO potential (Ref. 34) is now part of the open-source LAMMPS molecular dynamics package, which is available for download from [lammmps.sandia.gov](http://lammmps.sandia.gov).

\*ase@gatech.edu

†gchen2@mit.edu

- <sup>1</sup>D. G. Cahill *et al.*, *J. Appl. Phys.* **93**, 793 (2003).
- <sup>2</sup>A. Henry and G. Chen, *J. Comput. Theor. Nanosci.* **5**, 141 (2008).
- <sup>3</sup>K. E. Goodson and Y. S. Ju, *Annu. Rev. Mater. Sci.* **29**, 261 (1999).
- <sup>4</sup>D. Li *et al.*, *Appl. Phys. Lett.* **83**, 2934 (2003).
- <sup>5</sup>S. Berber, Y.-K. Kwon, and D. Tomanek, *Phys. Rev. Lett.* **84**, 4613 (2000).
- <sup>6</sup>P. Kim, L. Shi, A. Majumdar, and P. L. McEuen, *Phys. Rev. Lett.* **87**, 215502 (2001).
- <sup>7</sup>C. Yu *et al.*, *Nano Lett.* **5**, 1842 (2005).
- <sup>8</sup>A. Henry and G. Chen, *Phys. Rev. Lett.* **101**, 235502 (2008).
- <sup>9</sup>C. L. Choy *et al.*, *J. Polym. Sci., Part B: Polym. Phys.* **37**, 3359 (1999).
- <sup>10</sup>A. Henry and G. Chen, *Phys. Rev. B* **79**, 144305 (2009).
- <sup>11</sup>S. Shen *et al.*, *Nat. Nanotechnol.* **5**, 251 (2010).
- <sup>12</sup>J. F. Moreland, J. B. Freund, and G. Chen, *Nanoscale Microscale Thermophys. Eng.* **8**, 61 (2004).
- <sup>13</sup>E. Fermi, J. Pasta, and S. Ulam, Los Alamos Science Laboratory Report No. LA1940, 1955 (unpublished).
- <sup>14</sup>T. Prosen and D. K. Campbell, *Chaos* **15**, 015117 (2005).
- <sup>15</sup>D. K. Campbell, P. Rosenau, and G. M. Zaslavsky, *Chaos* **15**, 015101 (2005).
- <sup>16</sup>B. Li and J. Wang, *Phys. Rev. Lett.* **91**, 044301 (2003).
- <sup>17</sup>S. Lepri, R. Livi, and A. Politi, *Phys. Rev. E* **68**, 067102 (2003).
- <sup>18</sup>R. Livi and S. Lepri, *Nature (London)* **421**, 327 (2003).
- <sup>19</sup>S. Lepri, R. Livi, and A. Politi, *Anomalous Transport: Foundations and Applications* (Wiley-VCH, Wein, 2008).
- <sup>20</sup>E. Skow, *Mechanical Engineering* (Massachusetts Institute of Technology, Cambridge, 2007), p. 63.
- <sup>21</sup>D. B. Mergenthaler *et al.*, *Macromolecules* **25**, 3500 (1992).
- <sup>22</sup>D. L. Nika *et al.*, *Appl. Phys. Lett.* **94**, 203103 (2009).
- <sup>23</sup>S. Ghosh *et al.*, *Nature Mater.* **9**, 555 (2010).
- <sup>24</sup>A. A. Balandin *et al.*, *Nano Lett.* **8**, 902 (2008).
- <sup>25</sup>J. Hansen and I. McDonald, *Theory of Simple Liquids* (Academic Press, London, 1986).
- <sup>26</sup>G. P. Srivastava, *Physics of Phonons* (Adam Hilger, New York, 1990).
- <sup>27</sup>G. Chen, *Nanoscale Energy Transport and Conversion: A Parallel Treatment of Electrons, Molecules, Phonons, and Photons* (Oxford University Press, Oxford, 2005).
- <sup>28</sup>R. Hardy, *Phys. Rev.* **132**, 168 (1963).
- <sup>29</sup>J. Che *et al.*, *J. Chem. Phys.* **113**, 6888 (2000).
- <sup>30</sup>A. J. H. McGaughey and M. Kaviani, *Phys. Rev. B* **69**, 094303 (2004).
- <sup>31</sup>L. Sun and J. Murthy, *Appl. Phys. Lett.* **89**, 171919 (2006).
- <sup>32</sup>S. G. Volz, *Phys. Rev. Lett.* **87**, 074301 (2001).
- <sup>33</sup>D. W. Brenner *et al.*, *J. Phys.: Condens. Matter* **14**, 783 (2002).
- <sup>34</sup>S. Stuart, A. B. Tutein, and J. A. Harrison, *J. Chem. Phys.* **112**, 6472 (2000).
- <sup>35</sup>S. Plimpton, *J. Comput. Phys.* **117**, 1 (1995).
- <sup>36</sup>L. H. Sperling, *Introduction to Physical Polymer Science* (Wiley, Bethelhem, Pennsylvania, 2006).
- <sup>37</sup>L. Yin *et al.*, *Polymer* **44**, 6489 (2003).
- <sup>38</sup>J. Lukes and H. Zhong, *J. Heat Transfer* **129**, 705 (2007).
- <sup>39</sup>A. Henry and G. Chen, *Nanoscale Microscale Thermophys. Eng.* **13**, 99 (2009).
- <sup>40</sup>G. P. Srivastava, *J. Phys. Chem. Solids* **41**, 357 (1980).
- <sup>41</sup>D. A. Broido *et al.*, *Appl. Phys. Lett.* **91**, 231922 (2007).
- <sup>42</sup>M. Dove, *Introduction to Lattice Dynamics* (Cambridge University Press, New York, 1993).